Optics Communications 282 (2009) 3266–3269

Contents lists available at ScienceDirect

Optics Communications

journal homepage: www.elsevier.com/locate/optcom

Ultra-wideband single-polarization single-mode, high nonlinearity photonic crystal fiber

Lin An [a], Zheng Zheng [a,*], Zheng Li [a], Tao Zhou [b], Jiangtao Cheng [c]

[a] School of Electronic and Information Engineering, Beihang University, Beijing 100191, China
[b] Department of Physics, New Jersey Institute of Technology, Newark, NJ 07102, USA
[c] Department of Mechanical and Nuclear Engineering, Pennsylvania State University, University Park, PA 16802, USA

ARTICLE INFO

Article history:
Received 17 November 2008
Received in revised form 11 May 2009
Accepted 13 May 2009

Keywords:
Single-polarization
High nonlinearity
Photonic crystal fiber (PCF)

ABSTRACT

We report a novel design of photonic crystal fiber (PCF) with a rectangular array of four closely-spaced, highly elliptical air holes in the core region and a circular-air-hole cladding. The proposed PCF is able to support ultra-wideband single-polarization single-mode (SPSM) transmission from the visible band to the near infrared band. With the aid of the inner cladding formed by the central air holes, one polarization of the fundamental mode can be cut off at very short wavelengths and ultra-wideband SPSM propagation can be achieved. The inner cladding also suppresses the higher order modes and allows large air filling fraction in the outer cladding while the proposed fiber remains SPSM, which significantly reduces the mode effective area and the confinement loss. Our simulation results indicate that the proposed PCF has a 1540 nm SMSP range with <0.25 dB/km confinement loss and an effective area of 2.2 μm^2. Moreover, the group velocity dispersion (GVD) of the proposed PCF can also be tuned to be flat and near zero at the near infrared band (~800 nm) by optimizing the outer cladding structure, potentially enabling many nonlinear applications.

1. Introduction

In the past decade, single-polarization single-mode (SPSM) fibers have drawn increased interest because they support only one polarization state of the fundamental mode in many polarization sensitive applications. Due to their special characteristics such as high extinction ratio and no polarization mode coupling, they can be used as polarizing elements in high-power fiber lasers, fiber optic gyroscopes, and fiber sensors. A number of SPSM fibers based on photonic crystal fiber (PCF) structures have been proposed recently. Owing to the much higher index contrast in PCFs, wideband SPSM propagation can be realized. The previously reported designs of SPSM-PCF mainly rely on the asymmetric cladding structure and/or the stress-induced material birefringence to generate the large birefringence required by the SPSM fibers [1–6]. Many of these designs are focused on SPSMs with large mode effective areas that are useful in high-power systems [7,8]. On the other hand, novel optical fiber communication applications, such as parametric amplification, wavelength conversion and wavelength multicasting make use of fiber nonlinearity and prefer low-loss nonlinear SPSM fibers [9]. Nonlinear SPSM fibers could eliminate polarization-dependent noises and enhance interaction efficiency by aligning the polarization of the interacting waves in the same direction. Near-zero dispersions with small dispersion slopes would benefit applications like polarized supercontinuum generation [10]. For many of the conventional SPSM-PCF designs, small mode effective area and low confinement loss are difficult to achieve because the low air filling fraction of the cladding is required in their designs to realize both birefringence and fundamental mode cutoff. Recently we pointed out that large birefringence can be realized by introducing an array of circular or elliptical air holes in the core region of a PCF with relatively large air filling fractions of the cladding [11].

In this work, we demonstrate an ultra-wideband SPSM-PCF design with the core region containing a rectangular array of four highly elliptical air holes (to realize the fundamental mode cutoff) and an optimized circular-air-hole cladding with large air filling fraction (to reduce the mode effective area and the confinement loss). In contrast to the conventional SPSM-PCFs, the proposed PCF design exploits the novel four-hole inner cladding in the core region and enables the control of the fundamental mode cutoff by simply adjusting the spacings of the four holes. This four-hole arrangement in the inner core also relaxes requirements on the outer cladding design. As discussed in the following section, the inner cladding increases the air filling fraction of the core region and helps to cut off the fundamental *x*-polarized mode at very short wavelengths (in the visible band), and therefore enables an ultra-wide SPSM band. In this work, we show that the proposed design can provide a SPSM propagation over an ultra-wide wavelength

* Corresponding author.
E-mail address: zhengzheng@buaa.edu.cn (Z. Zheng).

0030-4018/$ - see front matter © 2009 Elsevier B.V. All rights reserved.
doi:10.1016/j.optcom.2009.05.033

range from 0.3 to 1.84 μm with the confinement loss as small as <0.25 dB/km. The mode effective areas at 800 and 1.55 μm are estimated to be 2.16 μm^2 and 3.56 μm^2, respectively. Such small mode areas can be leveraged to realize low bending losses. Compared to the previous design of high-birefringence fiber using elliptical holes at the core [11], the proposed SPSM-PCF design needs special care in designing the elliptic ratio and spacing of the central air holes. For the possible nonlinear applications, the proposed cladding modifications can achieve a flat and near zero group velocity dispersion (GVD) at ~800 nm.

2. Design and optimization of the PCF structure

Our SPSM-PCF design incorporates a rectangular array of four identical air holes in the core region [11], as shown in Fig. 1. These air holes are large enough to prohibit light propagation in them and behave like an inner cladding. To realize SPSM transmission, the elliptical ratio (ER) (a:b) of these holes, i.e. the ratio of the diameter a along the y-axis over the diameter b along the x-axis, and the spacings Λ_1 and Λ_2 between the holes in the y- and x-axis directions, need to be optimized. The cladding of the proposed PCF consists of a conventional hexagonal lattice of circular air holes with their pitch Λ being 2.2 μm. The background material of PCF is fused silica whose Sellmeier coefficients can be found in [12]. The field distribution and its effective modal effective indices (n_{eff}) are numerically simulated using a full-vector finite element method (FEM) simulator (COMSOL Multiphysics™), and the confinement loss, modal effective area A_{eff} and the fiber nonlinear coefficient γ of the modes are calculated [1,13].

2.1. Single-mode propagation

For traditional single-mode PCF designs, the air filling fraction (AFF) of the cladding are relatively low. When AFF is high, the effective refractive index of the cladding, i.e. that of the fundamental space-filling mode (FSM), becomes smaller and higher order modes can be supported. On the other hand, low AFF causes an increase in the mode effective area and the confinement loss. In our design, however, with the inner cladding of four elliptical holes, even though the AFF of the cladding is relatively high, the AFF of the core region is also increased. Thus, the effective mode indices supported in the core region are decreased, and the higher order modes can be suppressed at even higher AFF of the cladding. On the other hand, for the structures with circular inner holes or holes with small elliptical ratios, the edge-to-edge spacing between the inner air holes cannot be too small, otherwise the propagation of the fundamental mode at the center would be affected by the inner cladding. But for the PCFs using the central holes with large elliptical ratios, the minimal edge-to-edge spacing along the long axis between the holes can be reduced, and the fundamental mode can be still well confined to the center.

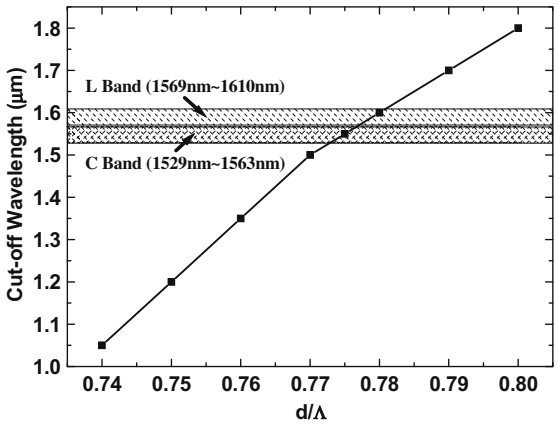

Fig. 2. Cut-off wavelength versus d/Λ.

To demonstrate that single-mode propagation can be realized even at large values of d/Λ, Fig. 2 gives the cut-off wavelengths of the 2nd-order mode at different d/Λ values. In these calculations, a and b are taken as 0.45Λ and 0.2Λ, respectively. As a result, our calculations show that Λ_2 should be larger than 0.45Λ to make the fundamental mode confined to the center, and here both Λ_1 and Λ_2 are taken as 0.55Λ. It can be seen that d/Λ can be as large as 0.77 while our proposed PCF still remains single-moded at the C and L bands. Fig. 3 shows the dispersion curves with $d/\Lambda = 0.77$ that indicates a cut-off wavelength of 1.5 μm for the 2nd-order mode. Other higher modes, including the x-polarized 2nd-order mode, are all cut off within the wavelength range in Fig. 3. For the fundamental mode, its x-polarized mode has a wider distribution in the x direction, and its n_{eff} is smaller than that of the y-polarized mode. The single-mode modal birefringence can reach as high as 0.02487 at 1.55 μm. The confinement loss is significantly reduced when d/Λ, i.e. AFF, is large. For either polarization, the highly elliptical holes greatly limit the field distribution along the direction of their short axis and the field is mainly distributed along the long axis of the holes.

2.2. Single-polarization propagation

To further cut off the x-polarized 1st-order mode to realize single-polarization propagation, we need to carefully adjust the elliptical ratio and the spacing of the inner holes as well as the AFF of the cladding.

Large birefringence between the two polarizations of the 1st-order mode is essential to achieve wideband SPSM. We found that,

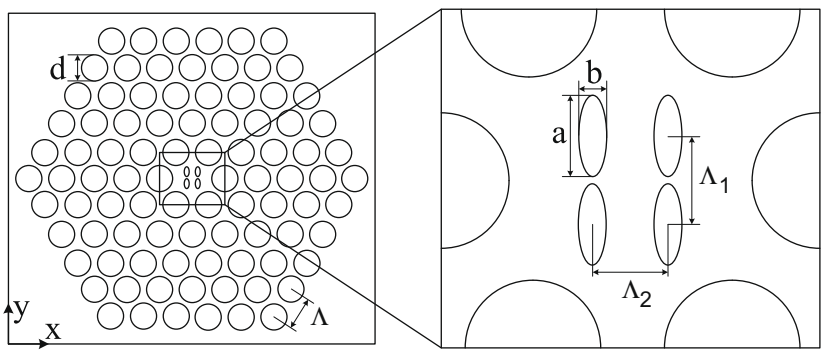

Fig. 1. Cross-sectional view of the proposed PCF.

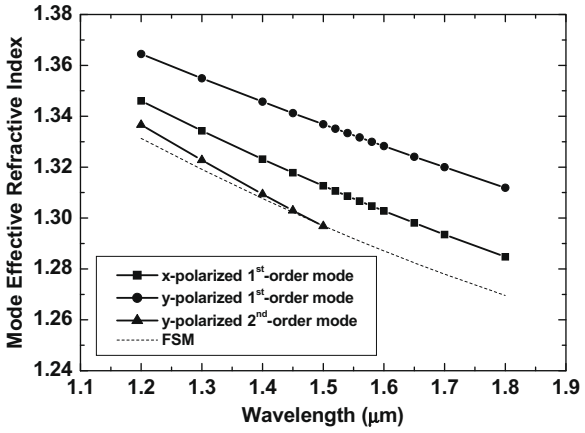

Fig. 3. Dispersion curves when d/Λ is 0.77.

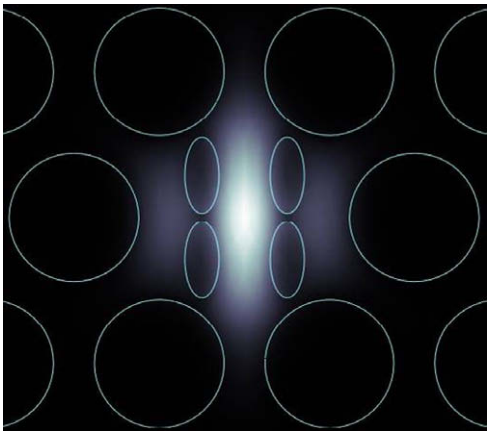

Fig. 4. Intensity distribution of *y*-polarized mode at 1.55 μm.

when the central air holes have large elliptical ratios, it is possible to simultaneously ensure a well-confined fundamental mode and provide large polarization birefringence because the minimal edge-to-edge distances in the long-axis direction of the holes can be much smaller than that in the short-axis direction. The birefringence is increased when Λ_1 is reduced. Thus, highly elliptical holes are very beneficial to our design because they allow smaller edge-to-edge spacings along the long axis between the holes as discussed in the previous section.

Closely spaced, highly elliptical air holes in the core region by themselves cannot guarantee the SPSM property. The AFF of the cladding also needs to be carefully designed. Besides the single-mode condition illustrated in Fig. 2, there are additional requirements on the upper limit of d/Λ. The resultant n_{eff} of FSM needs to be large enough to cut off the *x*-polarized mode. At certain conditions, even though the single-mode condition can be satisfied, the single-polarization condition can't. For example, the n_{eff} of FSM with $d/\Lambda = 0.77$ is so low that neither polarization of the fundamental mode gets cut off, even when both Λ_1 and Λ_2 are decreased to their minimum value of 0.45Λ. It is found that when d/Λ is set to be 0.76, the *x*-polarized mode can be cut off when both Λ_1 and Λ_2 are decreased to 0.5Λ. Further reduction of the AFF could increase the SPSM bandwidth at some expense of the confinement loss and mode effective area.

Within the compact spacings of the inner air holes, the effective indices of higher order modes are reduced and this reduction further suppresses the even higher modes. When Λ_1 and Λ_2 are decreased from 0.55Λ to 0.5Λ, the cut-off wavelength of the 2nd-order mode is extended towards the shorter wavelength side in comparison to that in Fig. 2.

In the above discussed configuration, i.e. $a = 0.45\Lambda$, $b = 0.2\Lambda$, $d/\Lambda = 0.76$ and $\Lambda_1 = \Lambda_2 = 0.5\Lambda$, the intensity distribution of the *y*-polarized fundamental mode under the SPSM condition is shown in Fig. 4.

To further identify the specific single-polarization requirement for the inner cladding structure, several PCF designs with different elliptical ratios have been examined at 1.55 μm. In these calculations, the d/Λ of the outer cladding is set to be 0.76, and we find that the ER should be larger than 2:1 to achieve the SPSM propagation, and both Λ_1 and Λ_2 should be no more than 0.5Λ.

We note that, in contrast to the birefringent fiber design in [11], where the elliptic ratio of the holes is relatively small (less than 2:1) and the spacings between the central holes need to remain large enough to keep the light confined to the fiber center, our current SPSM design can only be realized under a large elliptic ratio (larger than 2:1), and the spacing along the major axis direction needs to be small enough to cut off one polarization of the fundamental mode.

The key characteristics of the SPSM-PCF shown in Fig. 4 are examined in greater details here. Remarkably different from the conventional SPSM-PCFs, the 1st-order *x*-polarized mode in our design is cut off at 0.6 μm, even shorter than the 2nd-order y-polarized mode that is cut off at 1.1 μm (as shown in Fig. 5). Single-polarization multi-mode (SPMM) propagation exists within a wide wavelength range from 0.6 to 1.1 μm, and SPSM propagation can be achieved beyond 1.1 μm. The upper limit of the SPSM wavelength range is determined by the confinement loss herein, as the confinement loss of the 1st-order *y*-polarized mode increases rapidly at longer wavelengths. If we set the highest tolerable limit of the confinement loss at 0.25 dB/km, the SPSM range can reach from 1.1 to 1.62 μm, an ultra-wide 520 nm range covering both the 1.3 and 1.55 μm fiber communication windows.

In Fig. 5, the confinement losses are estimated based on the imagery part of the n_{eff}, which has been used as a performance indicator for the fiber design analysis, while the actual transmission loss of fabricated fiber will be significantly influenced by the fabrication process. It is also shown that a fairly flat negative chromatic dispersion distribution around the interested 1.55 μm wavelengths. In the C band (1529–1563 nm), the GVD only varies from −213 to −218 ps/(nm km). The mode effective area at 1.55 μm is calculated to be 6 μm^2, and the small mode area could enable lower bending losses.

2.3. Dispersion-optimized SPSM PCF

Since flat and near-zero GVD is preferred in many potential nonlinear applications it can be easily achieved by further modifi-

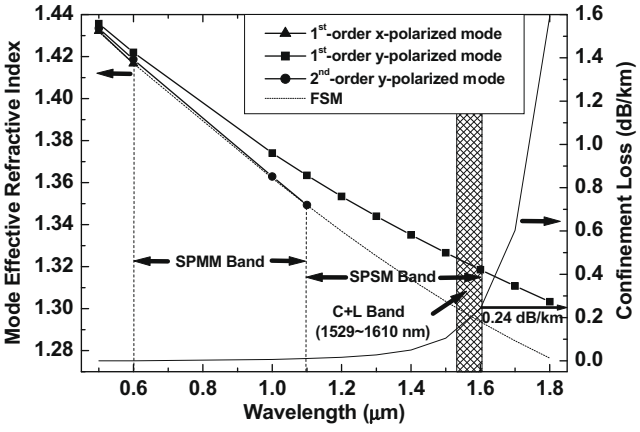

Fig. 5. Dispersion and confinement loss curves of the proposed PCF.

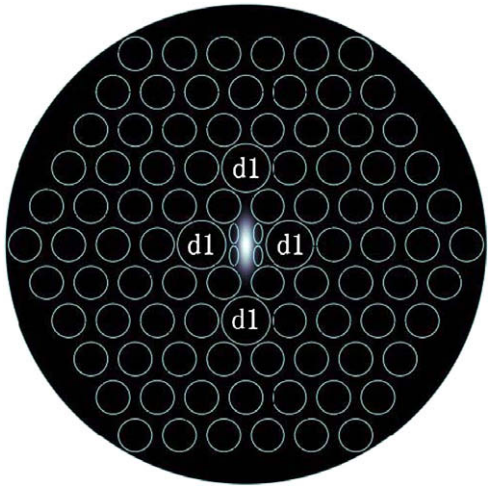

Fig. 6. Intensity distribution of *y*-polarized mode of the proposed dispersion-optimized SPSM PCF at 800 nm.

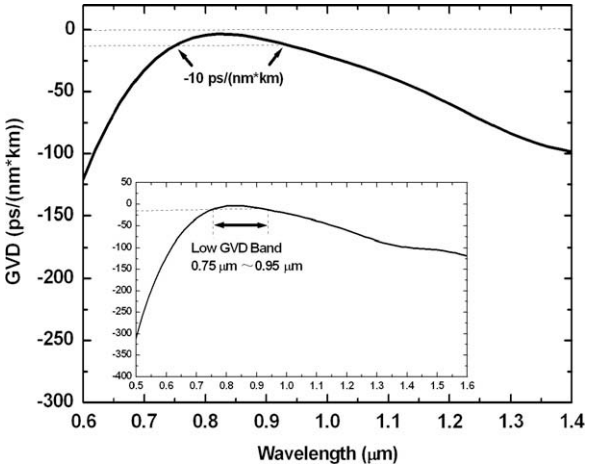

Fig. 7. Group velocity dispersion curve of the proposed dispersion-optimized SPSM PCF.

cations on the outer cladding, due to the four-hole inner cladding that relaxes the limitations on the outer cladding design.

One of the possible near-zero, dispersion-flattened PCF structures as well as the intensity distribution of the *y*-polarized fundamental mode at 800 nm is shown in Fig. 6. The diameter of the four big circular air holes $d1$ is 0.96Λ, while the other structure parameters are the same as those in Fig. 4. It can be seen from Fig. 6 that the mode field is more confined compared to that in Fig. 4 due to these larger cladding holes. The mode effective areas at 800 nm and 1.55 μm are estimated to be 2.16 and 3.56 μm^2, respectively. Considering the nonlinear refractive index (n_2) of the fused silica (fiber) as 3.2×10^{-20} m^2/W [14], the nonlinearity γ of the proposed PCF is estimated to be 116 W^{-1} km^{-1} at 800 nm. Also, the confinement loss is reduced, and the losses at 1.84 μm is calculated as 0.24 dB/km. Since the four big air holes help to suppress the higher order modes as well, the bandwidth of the SPSM propagation is extended to 1540 nm (0.3–1.84 μm), while the confinement loss is kept less than 0.25 dB/km. Fig. 7 shows the GVD curve within the SPSM band. The GVD value is within the range of 0∼−10 ps/(nm km) around 820 nm wavelength.

3. Discussions and conclusions

We propose a simple design of ultra-wideband SPSM-PCF with a rectangular array of four elliptical air holes in the core region, and along with an optimized circular-air-hole cladding both small mode size and near-zero dispersion can be realized. As a near-zero dispersion-flattened nonlinear SPSM fiber, the proposed PCF could be applied in various fields including parametric amplification, wide-band wavelength conversion, wavelength multicasting and supercontinuum generation. We believe that the stack-and-draw [15] or the die-cast method that is able to realize elliptical-hole and asymmetric PCF structures [16], can be used to fabricate such a structure. While the highly asymmetric mode shape of our proposed PCF design surely makes it more challenging to couple it with conventional optical fibers, such kind of highly birefringent PCFs have been widely proposed and implemented in the real applications and various schemes have been proposed to alleviate the problem [17].

Acknowledgement

The work was done at Beihang University and was supported by NSFC (60877054), NCET and PCSIRT, SEM, 973 Program (2009CB930701).

References

[1] K. Saitoh, M. Koshiba, IEEE Photon. Technol. Lett. 15 (October) (2003) 1384.
[2] H. Kubota et al., IEEE Photon. Technol. Lett. 16 (January) (2004) 182.
[3] M. Li et al., J. Lightw. Technol. 23 (November) (2005) 3454.
[4] J.R. Folkenberg et al., Opt. Lett. 30 (June) (2005) 1446.
[5] A. Petersson et al., Polarization properties of photonic crystal fibers, in: Proc. OFC' 2006, Anaheim, CA, 2006, OWA6.
[6] J. Ju et al., J. Lightw. Technol. 24 (February) (2006) 825.
[7] T. Schreiber et al., Opt. Express 13 (September) (2005) 7621.
[8] X. Chen et al., Opt. Express 16 (August) (2008) 12060.
[9] F. Zhang et al., J. Lightw. Technol. 25 (May) (2007) 1184.
[10] C. Xiong, W.J. Wadsworth, Opt. Express 16 (February) (2008) 2438.
[11] L. An et al., J. Lightw. Technol., doi: 10.1109/JLT.2008.2009074, in press.
[12] G.P. Agrawal, Fiber-Optic Communication Systems, third ed., John Wiley & Sons, Inc, New York, 2002 (Chapter 2).
[13] P. Sanchis et al., J. Lightw. Technol. 25 (May) (2007) 1298.
[14] R.W. Boyd, Nonlinear Optics, third ed., Academic Press, 2003, p. 212.
[15] M.J. Steel, R.M. Osgood, J. Lightw. Technol. 19 (April) (2001) 495.
[16] Z. Guiyao et al., Appl. Opt. 45 (June) (2006) 4433.
[17] S.G. Leon-Saval, T.A. Birks, et al., Opt. Lett. 30 (13) (2005) 1629. July.